ELSEVIER

Journal of Biomechanics 39 (2006) 1145–1152

JOURNAL OF BIOMECHANICS

www.elsevier.com/locate/jbiomech
www.JBiomech.com

Short communication

Predictions of co-contraction depend critically on degrees-of-freedom in the musculoskeletal model

Azim Jinha[1], Rachid Ait-Haddou[2], Walter Herzog*[,3]

Human Performance Laboratory, The University of Calgary, 2500 University Drive NW, Calgary, AB, Canada T2N 1N4

Accepted 5 March 2005

Abstract

In biomechanics, the calculation of individual muscle forces during movements is based on a model of the musculoskeletal system and a method for extracting a unique set of muscle forces. To obtain a unique set of muscle forces, non-linear, static optimisation is commonly used. However, the optimal solution is dependent on the musculoskeletal geometry, and single joints may be represented using one, two or three degrees-of-freedom. Frequently, a system with multiple degrees-of-freedom is replaced with a system that contains a subset of all the possible degrees-of-freedom. For example, the cat ankle joint is typically modelled as a planar joint with its primary degree-of-freedom (plantar–dorsiflexion), whereas, the actual joint has three rotational degrees-of-freedom. Typically, such simplifications are justified by the idea that the reduced case is contained as a specific solution of the more general case. However, here we demonstrate that the force-sharing solution space of a general, three degrees-of-freedom musculoskeletal system does not necessarily contain the solutions from the corresponding one or two degrees-of-freedom systems. Therefore, solutions of a reduced system, in general, are not sub-set solutions of the actual three degrees-of-freedom system, but are independent solutions that are often incompatible with solutions of the actual system. This result shows that representing a three degrees-of-freedom system as a one or two degrees-of-freedom system gives force-sharing solutions that cannot be extrapolated to the actual system, and vice-versa. These results imply that general solutions cannot be extracted from models with fewer degrees-of-freedom than the actual system. They further emphasise the need for precise geometric representation of the musculoskeletal system, if general force-sharing rules are to be derived.

Keywords: Muscle; Force-sharing; Optimisation; Movement control; Agonist; Antagonist

1. Introduction

The force-sharing problem remains one of the most fundamental and unsolved problems in biomechanics (Bernstein, 1967; Crowninshield and Brand, 1981b; Tsirakos et al., 1997). The aim of the force-sharing problem is to determine, experimentally or theoretically, the forces that individual muscles contribute to the movement of interest. Experimentally, the measurement of multiple muscle forces during movement remains technically challenging, and has only been performed in a handful of laboratories (Abraham and Loeb, 1985; Herzog and Leonard, 1991; Hodgson, 1983; Walmsley et al., 1978). Theoretically, predictions of individual muscle forces have been performed in abundance using a variety of techniques (Anderson and Pandy, 2001; Crowninshield and Brand, 1981a; Tsirakos et al., 1997).

In biomechanics, a common theoretical approach to the force-sharing problem has been the use of static optimisation (Ait-Haddou et al., 2004; Crowninshield and Brand, 1981a). Despite much criticism of the optimisation approach (Buchanan and Shreeve, 1996; Collins, 1995; Hatze, 1980, 2000), it is often argued that static optimisation is a viable method for estimating

*Corresponding author. Tel.: +403 220 3438; fax: +403 284 3553.
E-mail address: walter@kin.ucalgary.ca (W. Herzog).
[1]Natural Sciences and Engineering Research Council (NSERC) of Canada.
[2]The Pacific Institute for Mathematical Sciences (PIMS), Canada.
[3]The Canada Research Chair Programme, Canada.

0021-9290/$ - see front matter © 2005 Elsevier Ltd. All rights reserved.
doi:10.1016/j.jbiomech.2005.03.001

individual muscle forces (Chao, 2003; Li et al., 1999; Pandy, 2001; Prilutsky, 2000). Hence, the use of static optimisation for solving the force-sharing problem has not been abandoned since its inception approximately 30 years ago (e.g. Crowninshield and Brand, 1981a; Dul et al., 1984; Li et al., 1999; Penrod et al., 1974; Rasmussen et al., 2001; Rehbinder and Martin, 2001; Seireg and Arvikar, 1975; Tsirakos et al., 1997; van Dieën, 1997).

When modelling musculoskeletal geometries, two-dimensional approximations are often used to represent three-dimensional systems. This appears justified by the near two-dimensional movements of many everyday human activities, such as walking and bicycling. Similarly, two-dimensional musculoskeletal geometries have always been used when solving the force-sharing problem analytically, although three-dimensional solutions have been obtained using numerical approaches (Glitsch and Baumann, 1997; Li et al., 1999; van Dijke et al., 1999).

When considering the laws of co-contraction among antagonistic muscles using static optimisation, we discovered that general rules developed for two-dimensional systems did not hold for three-dimensional systems. For example, it is correct that in a planar system, single joint antagonists can never co-contract when using an optimisation approach of the generic form proposed by Crowninshield and Brand (1981a). However, as will be shown below, single joint antagonists can always co-contract in a three-dimensional system, except if they are exact antagonists; that is, if the angle between their moment-arm vectors is 180°. Although, it can be shown that, for this specific example, the two-dimensional result is contained in the three-dimensional solution, the question arose, is the two-dimensional solution *always* a subset of the solution of the corresponding three-dimensional system? In other words, is the prediction of antagonistic co-contraction dependent on the degrees-of-freedom of a system?

Here, we will demonstrate that the force-sharing solution space of a general three degrees-of-freedom musculoskeletal system does not necessarily contain the solutions from the corresponding one or two degrees-of-freedom approximations. The solutions of the three and two degrees-of-freedom system geometries are conceptually different. Therefore, any "*general*" rules derived from two-dimensional musculoskeletal geometries cannot necessarily be transferred into three-dimensional space and vice-versa. Similarly, any numerical solution of a two-dimensional system can conceptually differ from the solution using the actual three-dimensional geometry, even for "*almost*" planar (i.e. systems whose movements outside a single plane are small; e.g., the human ankle) system geometries. These results emphasise the importance of representing the actual musculoskeletal geometry as accurately as possible, and to avoid one or two degrees-of-freedom approximations of three degrees-of-freedom system geometries, even in cases where the system is considered "*nearly*" planar.

2. Methods

In order to study the prediction of individual muscle forces, illustrative models of the cat and human ankle joints are used. To study the effect of "*dimensionality*", we considered the cat ankle as having one, two and three rotational degrees-of-freedom. For the calculation of muscle forces, a general, non-linear, static-optimisation problem was formulated (Crowninshield and Brand, 1981a; Dul et al., 1984; Penrod et al., 1974; Tsirakos et al., 1997) to study predictions of co-contraction of pairs of antagonistic muscles. We then used the Karush–Kuhn–Tucker theorem (Clarke, 1989; Horst et al., 1995) for constrained optimisation to calculate the set of intersegmental moment vectors which guarantees co-contraction of a pair of muscles.

2.1. Model of the cat ankle joint

Three different methods of representing the cat ankle joint were developed. First, we developed a three-dimensional, three degrees-of-freedom model of the cat ankle joint (Fig. 1). Then, corresponding models with two and one degrees-of-freedom were developed by eliminating one, then two, degrees-of-freedom from the original model.

The original model consists of the three rotational degrees-of-freedom: (1) flexion/extension, (2) eversion/inversion, and (3) internal/external rotation (Fig. 1), and eleven muscles (Table 1). The moment-arm data were calculated from the maximum muscular torque and maximum muscle forces measured by Lawrence et al.

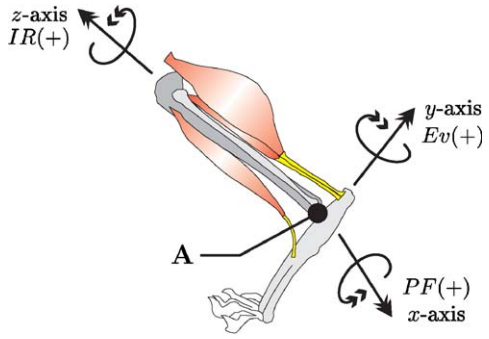

Fig. 1. Illustration of direction of positive rotations about the right cat-ankle joint center, A, in three-dimensional space. The directions of rotation about A are PF = plantar flexion (rotation about x), Ev = eversion (rotation about y); IR = internal rotation (rotation about z); PF, Ev, and IR describe positive rotations. Negative rotations about each of the three axis (x, y, and z) are refered to as dorsiflexion (DF), inversion (Inv), and external rotation (ER), respectively.

Table 1
Moment-arm vectors of the major muscles crossing the cat ankle joint calculated from data provided by Lawrence et al. (1993), and Sacks and Roy (1982)

i		Moment-arms			Weight factor (ω_i)
	Name	PF/DF (cm)	Ev/Inv (cm)	IR/ER (cm)	
1	Sol	1.63	0.08	−0.31	2.5
2	Tib A	−1.14	−0.30	0.37	5.78
3	Tib P	0.19	−0.21	0.76	0.75
4	Lat G	1.54	0.07	−0.32	8.29
5	Med G	1.90	0.08	−0.56	8.79
6	FHL	0.28	−0.02	0.09	3.93
7	FDL	0.14	−0.23	0.55	1.33
8	Per L	−0.45	0.30	−0.87	1.34
9	Per B	−0.37	0.42	−0.74	0.7
10	Per T	−0.74	−0.16	0.01	0.27
11	Per	−0.23	0.26	−0.75	2.3

The weight factor, ω, is the muscle's mass in grams taken from Lawrence et al. (1993), Sol—soleus (1); Tib A and Tib P—tibialis anterior (2) and posterior (3); Lat G and Med G—lateral (4) and medial (5) gastrocnemius; FHL—flexor hallucis longus (6); FDL—flexor digitorum longus (7); Per L, Per B and Per T—peroneus longus (8), brevis (9) and tertius (10); and Per—peroneus (11).

(1993), and Sacks and Roy (1982), respectively. The muscle torques published by Lawrence et al. (1993) were normalised relative to the cats' weights raised to the power $\frac{2}{3}$. Thus, moment-arm values were obtained from the normalised torque data by assuming an average mass of 4 kg, and dividing the normalised torques by the maximal force of each muscle (Sacks and Roy, 1982). The only exception to this procedure was the tibialis anterior, for which the above procedure gave unreasonable results. Therefore, a correction factor was used to give tibialis anterior a moment-arm vector which was consistent with that measured in our own experimental work.

2.2. Model of the human ankle joint

For the human ankle, a three-dimensional model was developed. From this three degrees-of-freedom model a second model with two degrees-of-freedom was obtained by eliminating one degree-of-freedom. The complete model of the human ankle consists of 12 muscles and three rotational degrees-of-freedom. The origin and insertion points of each muscle were obtained from Brand et al. (1982) and each muscle's physiological cross-sectional area was obtained from Brand et al. (1986). The muscles' lines of action were assumed to be straight, and moment-arm vectors about the ankle were calculated as an arbitrary vector from the ankle joint to a point on the line of action of the target muscle. The moment-arm vector of a muscle, $\boldsymbol{m}_i$, can be defined as

$$\boldsymbol{m}_i = \boldsymbol{r}_i \times \boldsymbol{e}_i. \tag{1}$$

Table 2 contains the moment-arm vectors of the 12 muscles crossing the human ankle.

2.3. The force-sharing problem

For the two models described above, the general relationship between muscle forces (f_i) and joint moment (b) can be written in matrix form as

$$\boldsymbol{A}\boldsymbol{f} = \boldsymbol{b}. \tag{2}$$

For the three degrees-of-freedom model, $\boldsymbol{A} = [m_1, \ldots, m_{11}]$ is a 3×11 or 3×12 moment-arm matrix for the cat and human ankle, respectively; $\boldsymbol{m}_i$ is the moment-arm vector of the ith muscle; $\boldsymbol{f} = [f_1, \ldots, f_m]^T$ is the vector of unknown muscle forces; and $\boldsymbol{b} = [b_1, b_2, b_3]^T$ is the intersegmental joint moment vector. The columns of matrix $\boldsymbol{A}$ can be interpreted as the moment-arm vector of each muscle, $\boldsymbol{m}_i$. Eq. (2) does not have a unique solution for the unknowns (f_i), and a particular solution can be obtained by formulating a non-linear, static optimisation problem (Ait-Haddou et al., 2004; Crowninshield and Brand, 1981b; Tsirakos et al., 1997).

2.4. Optimisation and prediction of co-contraction

The general static optimisation problem takes the form

$$\begin{aligned} &\text{minimise :} \quad \phi(\boldsymbol{f}) = \sum_{i=1}^{N} \left(\frac{f_i}{\omega_i}\right)^{\alpha}, \\ &\text{subject to :} \quad \boldsymbol{A}\boldsymbol{f} = \boldsymbol{b} \quad \text{and} \quad f_i \geqslant 0, \end{aligned} \tag{3}$$

where ω_i are generic weighting factors, and the constraints represent the equations of mechanical equilibrium and the fact that muscles can only produce positive (tensile) forces. The optimisation problem in Eq. (3) is non-linear, and convex for $\alpha > 1$ (Herzog and

Table 2
Moment-arm vectors of the major muscles crossing the human ankle joint. The weight factor, ω, is the physiological cross-sectional area of the muscle

i		Moment-arms			Weight factor (ω_i)
	Name	PF/DF (cm)	Ev/Inv (cm)	IR/ER (cm)	
1	Sol	3.54	−0.49	−0.05	15.54
2	Tib A	−2.34	2.09	−0.07	4.48
3	Tib P	0.21	2.74	0.21	3.21
4	Med G	1.89	−1.81	1.43	4.78
5	Lat G	2.09	−1.47	1.12	9.4
6	FHL	8.21	1.33	1.22	3.96
7	FDL	0.71	2.17	0.27	1.13
8	Per L	0.99	−2.43	−0.12	3.96
9	Per B	0.88	−2.7	−0.36	2.8
10	Per T	−2.06	−0.9	−0.43	1.74
11	EDL	−2.69	0.34	−0.26	2.41
12	EHL	−2.75	1.03	−0.1	1.2

Sol—soleus (1); Tib A and Tib P—tibialis anterior (2) and posterior (3); Lat G and Med G—lateral (4) and medial (5) gastrocnemius; FHL—flexor hallucis longus (6); FDL—flexor digitorum longus (7); Per L, Per B and Per T—peroneus longus (8), brevis (9) and tertius (10); EDL—extensor digitorum longus (11); and EHL—extensor hallucis longus (12).

Binding, 1993), therefore, if a solution exists it will be unique (Horst et al., 1995). A solution will always exist if the intersegmental moment vector, $\boldsymbol{b}$, is contained within the convex cone generated by the moment-arm vectors of the model.

Since Eq. (3) is a convex optimisation problem, the Karush–Kuhn–Tucker theorem gives the necessary and sufficient conditions for optimality (Clarke, 1989; Horst et al., 1995). These conditions, for each i, are

$$\alpha\frac{f_i^{\alpha-1}}{\omega_i^{\alpha}} = \langle \boldsymbol{m}_i, \boldsymbol{\lambda}\rangle + \mu_i,\ \mu_i f_i = 0 \quad \text{and} \quad \mu_i \geqslant 0. \tag{4}$$

We define a muscle to be active when $f_i > 0$, and silent when $f_i = 0$. In this case, the conditions in Eq. (4) give that a muscle is active if $\langle \boldsymbol{m}_i, \boldsymbol{\lambda}\rangle > 0$. Similarly, two muscles (i and j) are predicted to co-contract if

$$\boldsymbol{\lambda} \in \mathscr{C} = \{\boldsymbol{\lambda} | \langle \boldsymbol{\lambda}, \boldsymbol{m}_i\rangle > 0 \quad \text{and} \quad \langle \boldsymbol{\lambda}, \boldsymbol{m}_j\rangle > 0\}. \tag{5}$$

For a specific $\boldsymbol{\lambda} \in \mathscr{C}$, the corresponding intersegmental moment vector, $\boldsymbol{b}$, can be calculated in the following manner. First, the set of individual muscle forces are a function of $\boldsymbol{\lambda}$, i.e.

$$f_i = \begin{cases} \left[\frac{\omega_i^{\alpha}}{\alpha}\langle \boldsymbol{\lambda}, \boldsymbol{m}_i\rangle\right]^{1/\alpha-1} & \text{if } \langle \boldsymbol{m}_i, \boldsymbol{\lambda}\rangle > 0, \\ 0 & \text{otherwise.} \end{cases} \tag{6}$$

Once the muscle forces are determined from $\boldsymbol{\lambda}$, the corresponding intersegmental moment, $\boldsymbol{b}$, is calculated as

$$\boldsymbol{b} = \sum_{i=1}^{11} f_i \boldsymbol{m}_i. \tag{7}$$

The set $\mathscr{C}$ is a convex cone (the intersection of two half-spaces); if $\boldsymbol{\lambda} \in \mathscr{C}$, then $a\boldsymbol{\lambda} \in \mathscr{C}$ for all $a > 0$. Now, each $\boldsymbol{\lambda} \in \mathscr{C}$ can be mapped to a unique intersegmental moment, $\boldsymbol{b}$. This mapping is defined by Eqs. (5)–(7), and it is continuous. Therefore, the set of intersegmental moments associated with $\mathscr{C}$ is a connected set of vectors containing all the intersegmental moments for which the optimisation problem in Eq. (3) predicts co-contraction between muscles i and j. Also, the region of co-contraction is independent of the magnitude of the intersegmental moment. Therefore, these regions are represented by sections of the unit circle.

3. Results

It has been stated that static optimisation, of the form presented in Eq. (3), cannot predict co-contraction for a pair of antagonistic muscles crossing a single joint (Herzog and Binding, 1992; Hughes and Chaffin, 1988). However, this claim was made for a planar system with joints having a single rotational degree-of-freedom. If at least one other rotational degree-of-freedom is included in a model, then it is possible for the static optimisation to predict co-contraction of a pair of antagonistic muscles for a specific set of directions of the intersegmental moment vector (Ait-Haddou et al., 2004). The only case for which co-contraction cannot be predicted for any intersegmental moment vector is if the moment-arm vectors of two muscles are exact antagonists; i.e., $\boldsymbol{m}_i = -\beta\boldsymbol{m}_j$ ($\beta \geqslant 0$), and then the set $\mathscr{C}$ in Eq. (5) is empty (Ait-Haddou et al., 2004).

In the two degrees-of-freedom model of the cat ankle, we added eversion/inversion to the one degree-of-freedom model. With two degrees-of-freedom, each pair of antagonistic muscles was predicted to co-contract, because no pair of two muscles in the model is exactly antagonistic. Therefore, for each pair of muscles, it is

possible to find a set of intersegmental moments for which that pair is predicted to co-contract. For example, consider two pairs of antagonistic muscles (Fig. 2): (1) soleus and tibialis anterior (Sol–TibA) and (2) tibialis posterior and peroneus longus (TibP–PerL). Each region of co-contraction for these muscles is a convex cone, as expected. However, note that the size of the two regions of co-contraction is not comparable; Sol–TibA has a much greater region of co-contraction than TibP–PerL. Therefore, it is more likely to predict co-contraction for some antagonistic pairs of muscles than others. The small region of co-contraction for TipP–PerL might be missed by numerical analysis.

By adding internal/external rotation to the two degrees-of-freedom model, we recover the original model of the cat ankle joint in Table 1. Regions of co-contraction are now connected cones in the three-dimensional joint configuration space and can be represented conveniently using two spherical angles (θ and ϕ in Fig. 3). For spherical coordinates, a moment-arm vector can be written as

$$\boldsymbol{m} = ||\boldsymbol{m}|| (\cos\,\theta\,\sin\,\phi,\ \sin\,\theta\,\sin\,\phi,\ \cos\,\phi).$$

In Fig. 3, we consider the region of co-contraction of the two pairs of antagonistic muscles, Sol–TibA (Fig. 3A) and TibP–PerL (Fig. 3B). In the case of the Sol–TibA pair of antagonistic muscles, the region of co-contraction calculated with the two degrees-of-freedom model is partially contained within the region calculated using the three degrees-of-freedom model. Now consider the TibP–PerL pair of antagonistic muscles. For this pair of muscles the region of co-contraction for the two degrees-of-freedom system is completely outside the region calculated using the three degrees-of-freedom model. Although not shown, the same result is obtained for each pair of antagonistic muscles in the model.

For the model of the human ankle we chose the same two pairs of antagonistic muscles, as used above for the cat ankle, the Sol–TibA pair, and the TibP–PerL pair, to illustrate selected results. For the two degrees-of-freedom model (Fig. 4), the region of co-contraction is a

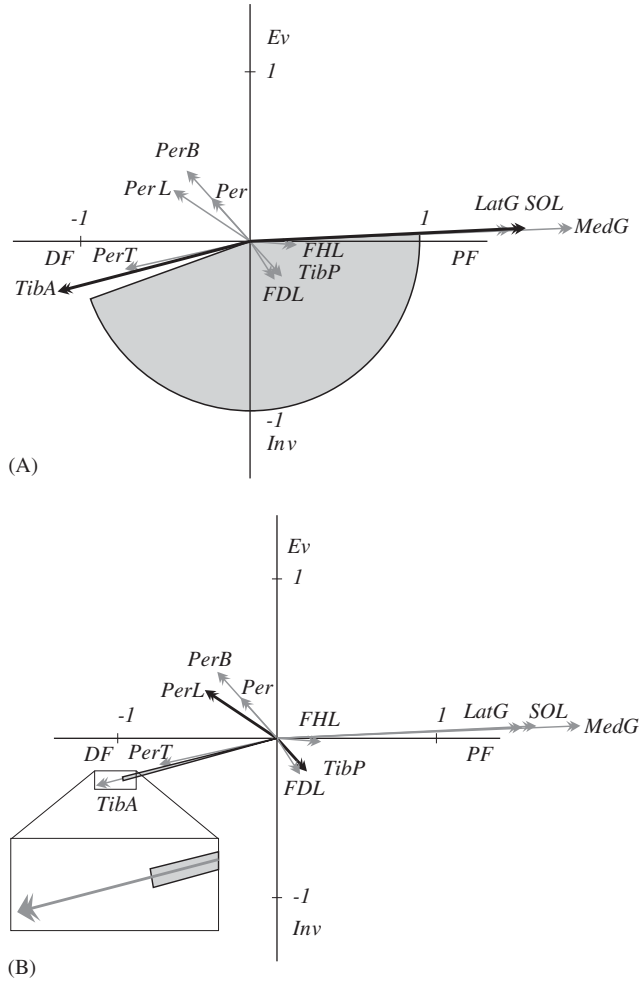

Fig. 2. Moment-arm vectors for the simplified two degrees-of-freedom model along with the regions of co-contraction (shaded areas) of (A) soleus/tibialis anterior and, (B) tibilis posterior/peroneus longus for the model of the cat ankle joint. Because the region of co-contraction is a convex cone, it is represented as a portion of the unit circle.

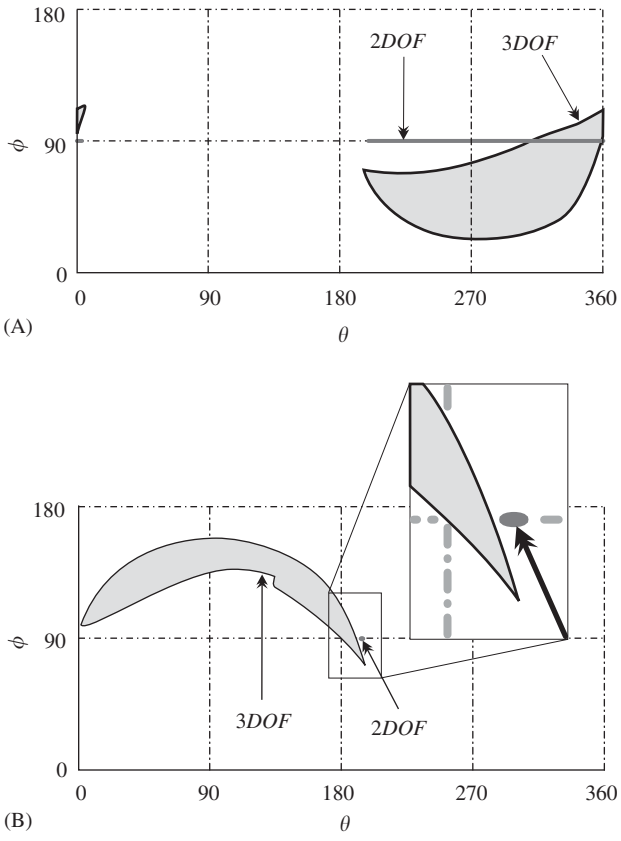

Fig. 3. Comparison of the regions of co-contraction of (A) soleus/tibialis anterior and (B) tibialis posterior/peroneus longus for the three degrees-of-freedom (3DOF), and the two degrees-of-freedom (2DOF) model of the cat ankle joint. The spherical angles θ and ϕ of the moment vector are plotted.

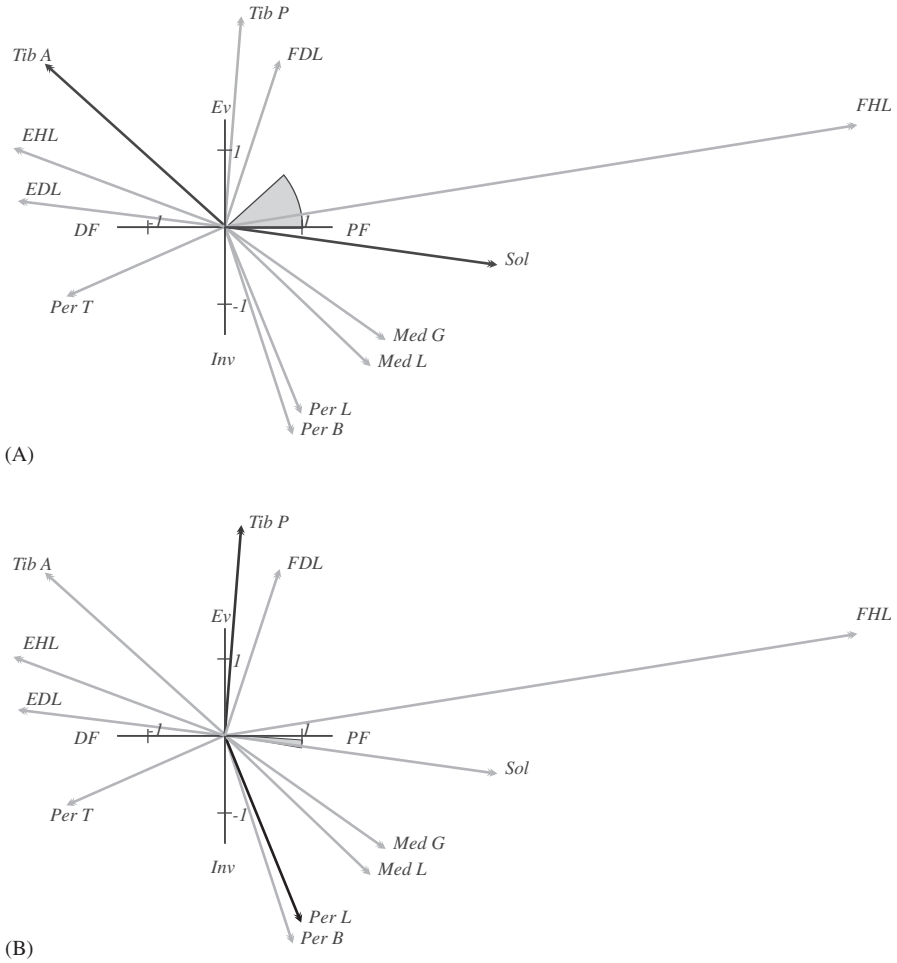

Fig. 4. Moment-arm vectors for the simplified two degrees-of-freedom model along with the regions of co-contraction (shaded areas) of (A) soleus/tibialis anterior and, (B) tibilis posterior/peroneus longus for the human ankle joint model. Because the region of co-contraction is a convex cone, it is represented as a portion of the unit circle.

convex cone for both muscle pairs. For the Sol–TibA (Fig. 4A), the region is located in the quadrant represented by plantar flexion and eversion. Because of the different distribution of muscles in the cat and human ankle models, the size of the region of co-contraction for Sol–TibA is greater for the cat than the human model. Also, the two regions of co-contraction occupy different parts of the moment-arm space. For the cat ankle model, the region is located in the lower half plane with an inversion moment, whereas for the human model, it is located in the upper half plane with an eversion moment. For the second pair of antagonists, TibP–PerL (Fig. 4B), the region of co-contraction is smaller than that for the Sol–TibA pair. For the two degrees-of-freedom models, the region of co-contraction lies within the convex cone generated by the pair of antagonistic muscles.

For the three degrees-of-freedom model of the human ankle, the region of co-contraction for both pairs of antagonistic muscles becomes larger than that for the two degrees-of-freedom model (Fig. 5), and the region of co-contraction is again a connected cone. For Sol–TibA pair (Fig. 5A), the region of co-contraction contains moment directions not included in the solution of the two degrees-of-freedom case.

For the TibP–PerL pair (Fig. 5B), the region of co-contraction is not much different than that for the two degrees-of-freedom case. It is slightly greater, but it contains the same moment directions as the two degrees-of-freedom case. Most solutions of the three degrees-of-freedom models contained moment directions that were not part of the two degrees-of-freedom results.

4. Discussion

Over the past 30 years, approximately 100 papers using static optimisation as a method for solving the force-sharing problem in biomechanics have been published (see reviews Crowninshield and Brand,

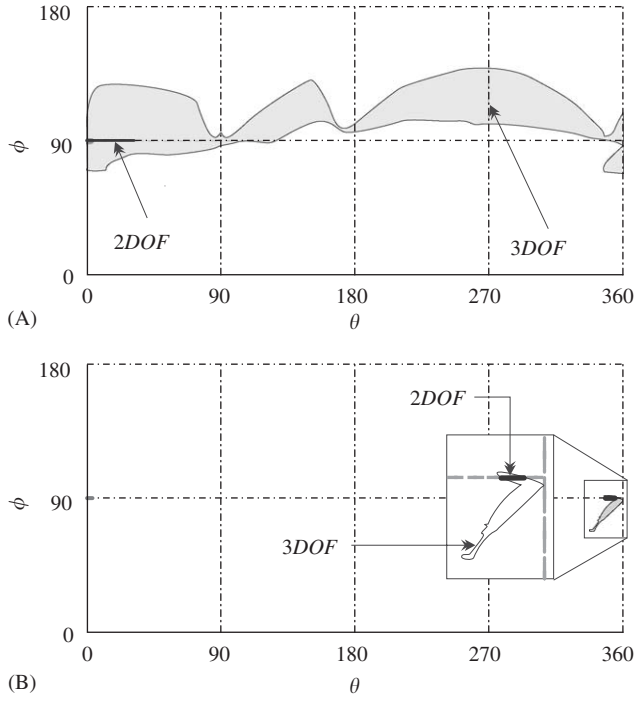

Fig. 5. Comparison of the regions of co-contraction of (A) soleus/tibialis anterior and (B) tibialis posterior/peroneus longus for the three degrees-of-freedom (3DOF), and the two degrees-of-freedom (2DOF) model of the human ankle joint. The spherical angles θ and ϕ of the moment vector are plotted.

1981b; Herzog, 1996). Solutions were obtained numerically for some large scale models or analytically for small scale, idealised models. Recently, we discovered a generalised solution for the force-sharing problem using generic optimisation approaches of the form shown in Eq. (3) (Ait-Haddou et al., 2004) that is independent of the system geometry. Here, we use this approach to test whether solutions of an original, three-dimensional system (that maybe nearly planar) contain the solutions of reduced two or one degrees-of-freedom models as sub-sets of the original solution. We demonstrate that this is not the case.

The implications of this result are as straightforward as they are important: the solutions of a reduced system are not necessarily contained in the solution space of the original model. Therefore, the force-sharing behaviour predicted with the original model and a reduced model of any kind may not match, and predictions of a reduced sub-system cannot be generalised to the original system or vice-versa. Therefore, any interpretation of numerical results, or conclusions of analytical analysis using one or two degrees-of-freedom models of a three degrees-of-freedom anatomical joint must be considered with great care, and should be viewed with the knowledge that these solutions may not approach those of the "*real*" three dimensional joint analysis.

If we assume for a moment that individual force control obeys an optimisation law, as assumed when using optimisation techniques, our result suggests that adequate muscle force-sharing predictions are only possible with models that accurately reflect the musculoskeletal geometry, and that contain a full representation of all rotational degrees-of-freedom. Therefore, claims of adequate (or inadequate) muscle force predictions must be carefully evaluated based on the model used to represent the actual musculoskeletal geometry, and should only be interpreted within the musculoskeletal geometry that was used for analysis, except if the results are proven to be generalisable across musculoskeletal geometries and are shown to be valid independent of the system's degrees-of-freedom.

Biomechanical analysis of human, or animal, movement are often performed using planar systems. Depending on the purpose of the study, such planar approaches may be perfectly acceptable. However, here we demonstrate that such an approach cannot be successful in predicting individual muscle forces accurately for three-dimensional joints, even if the projection of the actual geometry was done perfectly, and the optimisation scheme precisely reflected how muscle forces are controlled.

Previous analyses of the effects of musculoskeletal geometry on the predicted muscle forces using optimisation have demonstrated that small changes in the size or moment-arm of muscles might change the solution space in the sense that silent muscles might become active and vice-versa (Brand et al., 1986; Herzog and Binding, 1993), and that the number of degrees-of-freedom of the system determines if antagonistic activity is possible (Herzog and Binding, 1992). Here, we add an important aspect to the behaviour of optimisation approaches of the form shown in Eq. (3), the idea that the solution space for co-contraction of antagonistic muscles critically depends on the degrees-of-freedom of a system whose geometry is derived from projection of the original three-dimensional joint into the corresponding two-or one-dimensional sub-space, and that the solution space of the three-dimensional system may not contain all or parts of the solution space of the redundant systems.

References

Abraham, L., Loeb, G., 1985. The distal hind-limb musculature of the cat. Experimental Brain Research 58, 583–593.

Ait-Haddou, R., Jinha, A., Herzog, W., Binding, P., 2004. Analysis of the force-sharing problem using an optimization algorithm. Mathematical Biosciences 191 (2), 111–122.

Anderson, F., Pandy, M., 2001. Dynamic optimization of human walking. Journal of Biomedical Engineering 123, 381–390.

Bernstein, N., 1967. The coordination and regulation of movements. Pergamon, Oxford.

Brand, R., Crowninshield, R., Wittstock, C., Pedersen, D., Clark, C., van Krieken, F., 1982. A model of lower extremity muscular anatomy. Journal of Biomechanical Engineering 104, 304–310.

Brand, R., Pedersen, D., Friederich, J., 1986. The sensitivity of muscle force predictions to changes in physiologic cross-sectional area. Journal of Biomechanics 19 (8), 589–596.

Buchanan, T., Shreeve, D., 1996. An evaluation of optimization techniques for the prediction of muscle activation patterns during isometric tasks. Journal of Biomechanical Engineering 118 (4), 565–574.

Chao, E., 2003. Graphic based musculoskeletal model for biomechanical analyses and animation. Medical Engineering and Physics 25, 201–212.

Clarke, F., 1989. Optimization and nonsmooth analysis. Université de Montréal, Montréal, PQ.

Collins, J., 1995. The redundant nature of locomotor optimization laws. Journal of Biomechanics 28 (3), 251–267.

Crowninshield, R., Brand, R., 1981a. A physiologically based criterion of muscle force prediction in locomotion. Journal of Biomechanics 14 (11), 793–801.

Crowninshield, R., Brand, R., 1981b. The prediction of forces in joint structures: distribution of intersegmental resultants. Exercise and Sports Sciences Reviews 9, 159–181.

Dul, J., Townsend, M., Shiavi, R., Johnson, G., 1984. Muscular synergism—I. On criteria for load sharing between synergistic muscles. Journal of Biomechanics 17 (9), 663–673.

Glitsch, U., Baumann, W., 1997. The three-dimensional determination of internal loads in the lower extremity. Journal of Biomechanics 30 (11/12), 1123–1131.

Hatze, H., 1980. Neuromuscular control systems modeling: a critical survey of past developments. IEEE Transactions on Automatic Control AC-25, 375–385.

Hatze, H., 2000. The inverse dynamics problem of neuromuscular control. Biological Cybernetics 82 (2), 133–141.

Herzog, W., 1996. Force-sharing among synergistic muscles: theoretical considerations and experimental approaches. Exercise and Sports Sciences Reviews 24, 173–202.

Herzog, W., Binding, P., 1992. Predictions of antagonistic muscular activity using non-linear optimization. Mathematical Biosciences 111 (2), 217–229.

Herzog, W., Binding, P., 1993. Co-contraction of pairs of antagonistic muscles: analytical solution for planar static non-linear optimization approaches. Mathematical Biosciences 118 (1), 83–95.

Herzog, W., Leonard, T., 1991. Validation of optimization models that estimate the forces exerted by synergistic muscles. Journal of Biomechanics 24 (Suppl. 1), 31–39.

Hodgson, J., 1983. The relationship between soleus and gastrocnemius muscle activity in conscious cats—a model for motor unit recruitment? Journal of Physiology 337, 553–562.

Horst, R., Pardalos, P., Thoai, N., 1995. Introduction to Global Optimization. Kluwer Academic Publishers, Dordrecht, The Netherlands.

Hughes, R., Chaffin, D., 1988. Conditions under which optimization models will not predict coactivation of antagonist muscles. Proceedings of the American Society of Biomechanics 12, 69–70.

Lawrence, J., Nichols, T., English, A., 1993. Cat hindlimb muscles exert substantial torques outside the sagittal plane. Journal of Neurophysiology 69 (1), 282–285.

Li, G., Kaufman, K., Chao, E., Rubash, H., 1999. Prediction of antagonistic muscle forces using inverse dynamic optimization during flexion/extension of the knee. Journal of Biomechanical Engineering 121, 316–322.

Pandy, M., 2001. Computer modeling and simulation of human movement. Annual Reviews in Biomedical Engineering 3, 245–273.

Penrod, D., Davy, D., Singh, D., 1974. An optimization approach to tendon force analysis. Journal of Biomechanics 7, 123–129.

Prilutsky, B., 2000. Coordination of two- and one-joint muscles: functional consequences and implications for motor control. Motor Control 4, 1–44.

Rasmussen, J., Damsgaard, M., Voigt, M., 2001. Muscle recruitment by the min/max criterion—a comparative numerical study. Journal of Biomechanics 34, 409–415.

Rehbinder, H., Martin, C., 2001. A control theoretic model of the forearm. Journal of Biomechanics 34, 741–748.

Sacks, R., Roy, R., 1982. Architecture of the hind limb muscles of cats: functional significance. Journal of Morphology 173 (2), 185–195.

Seireg, A., Arvikar, R., 1975. The prediction of muscular load sharing and joint forces in the lower extremity during walking. Journal of Biomechanics 8, 89–102.

Tsirakos, D., Baltzopoulos, V., Bartlett, R., 1997. Inverse optimization: functional and physiological considerations related to the force-sharing problem. Critical Reviews in Biomedical Engineering 25 (4–5), 371–407.

van Dieën, J., 1997. Are recruitment patterns of the trunk musculature compatible with a synergy based on the maximization of endurance. Journal of Biomechanics 30 (11/12), 1095–1100.

van Dijke, G., Snijders, C., Stoeckart, R., Stam, H., 1999. A biomechanical model on muscle forces in the transfer of spinal load to the pelvis and legs. Journal of Biomechanics 32, 927–933.

Walmsley, B., Hodgson, J., Burke, R., 1978. Forces produced by medial gastrocnemius and soleus muscles during locomotion in freely moving cats. Journal of Neurophysiology 41 (5), 1203–1216.